

Parenteral Peptide Formulations: Chemical and Physical Properties of Native Luteinizing Hormone-Releasing Hormone (LHRH) and Hydrophobic Analogues in Aqueous Solution

Michael F. Powell,^{1,2} Lynda M. Sanders,¹
Alan Rogerson,¹ and Vicki Si¹

Received January 16, 1991; accepted May 6, 1991

The degradation of native LHRH in aqueous buffers of pH ~1–10 obeyed the rate equation, $k_{\text{obs}} = k_{\text{H}^+}a_{\text{H}^+} + k_{\text{o}} + k_{\text{HO}^-}(a_{\text{HO}^-})^x$, where x at 60–100°C was ~0.64 and temperature independent. Extrapolation to 25°C using the Arrhenius equation and secondary rate constants showed that native LHRH is reasonably stable at pH 5.4, giving a shelf life (t_{90}) of approximately 5 years. Regarding physical properties, hydrophobic LHRH analogues nafarelin and detirelix were found to be surface active as demonstrated by a decrease in apparent surface tension with increased peptide concentration. The CMC for detirelix at pH 7.4 was determined to be 5.3×10^{-4} M (0.88 mg/ml), and that for nafarelin, >2 mg/ml. At higher concentrations (~4–8 mg/ml), nafarelin and detirelix formed nematic liquid crystals of undulose extinction (birefringence, <0.001). The thermodynamic stability of these peptide liquid crystals was probed by determining their melting points (T_{cm}) in the presence of propylene glycol, a solvent which proved to be efficacious at suppressing gelation and at destabilizing liquid crystals as measured by a reduction in T_{cm} .

KEY WORDS: peptide stability; liquid crystal formation; birefringence; surface tension; luteinizing hormone-releasing hormone (LHRH); hydrolysis; aggregation; micelles; surface activity.

INTRODUCTION

The low oral bioavailability of most peptides and proteins has provided a compelling driving force for parenteral delivery. Unfortunately, the parenteral formulation of peptides and proteins is far from trivial. For example, certain peptides, such as the hydrophobic LHRH analogues nafarelin and detirelix (Fig. 1), adhere tenaciously to glass and other surfaces at low concentrations (1). At higher concentrations, aqueous formulations of nafarelin or detirelix undergo peptide aggregation and solution gelation resulting in compromised physical stability (2). Furthermore, although the chemical stability of selected hydrophobic LHRH analogues is well understood (3–9), there exist only limited chemical stability data for the parent compound, native LHRH.

Herein we report some of the chemical and physical

properties of nafarelin and detirelix that are pertinent to their parenteral formulation, as well as some stability data on native LHRH for comparison. We have determined the chemical stability of native LHRH with respect to temperature and pH, as well as probed the physical stability of hydrophobic LHRH analogues, by measuring the surface activity of these amphiphilic peptides and by directly measuring the stability of peptide aggregates at higher temperatures. The second paper in this series will report on the effect of pH, added counterions and excipients on peptide aggregation and physical stability (10).

EXPERIMENTAL

Materials

Nafarelin and detirelix (both as the diacetate salt) were synthesized and assayed by the Institute of Organic Chemistry (Syntex Research). Native LHRH (as the acetate salt) was purchased from Sigma and used without further purification. Buffer solutions and added cosolvents were prepared from reagent grade or USP-grade chemicals. HPLC-grade acetonitrile and water purified by filtration and ion exchange (Nanopure) were used in the mobile phase.

Apparatus

Reversed-phase chromatography of native LHRH was carried out using an HPLC system consisting of a Waters Model 712 Wisp autoinjector, a Waters Model 45 pump, a Waters Model 730 data module, and a Waters Model 450 spectrophotometric detector. A 250 × 4.6-mm Altex Ultra-sphere ODS column was used for analysis. pH's were determined using a Radiometer PHM 64 pH meter and a Radiometer GK2401C combination electrode calibrated at the solution temperature.

HPLC Conditions

A linear response ($\pm 1\%$) was obtained throughout the range of 0.005–5 μg LHRH injected. The separation of LHRH from its degradation products was achieved using the following conditions: mobile phase, water: acetonitrile (82:18, v/v) buffered with 0.2 M phosphate (pH 3); flow rate, 1.2 ml/min; detection, 210 nm; injection volume, 50 μl ; and typical LHRH retention time, 15 min. Stability specificity of this method was demonstrated by the following: (i) apparent pseudo-first-order decay of LHRH to <5% drug remaining; (ii) the spectral similarity obtained for early, middle, and late peak splices; and (iii) the lack of degradation product peaks at or near the LHRH peak when the mobile phase was varied.

Reaction Kinetics

The buffer concentration used in these experiments (except for HCl solutions) was held at 0.01 M to minimize buffer catalysis; the ionic strength was constant at $\mu = 0.15$ (KCl). LHRH acetate was added to make the final drug concentration 25 $\mu\text{g}/\text{ml}$ ($\sim 2 \times 10^{-5}$ M) and the pH's of each solution were determined at 25, 60, and 80°C. The pH's at 100°C were

¹ Institute of Pharmaceutical Sciences, Syntex Research, Palo Alto, California.

² To whom correspondence should be addressed at Genentech, Inc., 460 Pt. San Bruno Boulevard, South San Francisco, California 94080

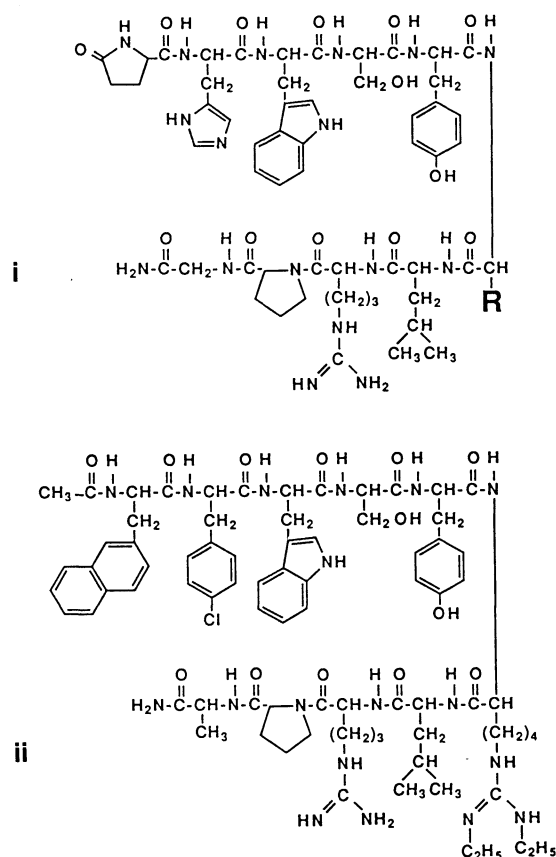


Fig. 1. Structure of (i) native LHRH ($R = H$), nafarelin ($R = 2$ -naphthylmethyl), and (ii) detirelix.

extrapolated by linear least-squares analysis of $1/T(K^{-1})$ versus pH. The reaction solutions were then transferred to several 1-ml clear glass vials (treated, type A), flame-sealed, and incubated at 60, 80, or 100°C. At known time intervals samples were removed and immediately frozen at -20°C . Typically 8–10 samples were taken per kinetic run. Upon removal of the last sample the stored solutions were allowed to warm to room temperature, and then all samples were analyzed on the same day. Peak area integration values were used directly when fitting the data to first order kinetics; typically reactions were followed for two to five half-lives.

Physical Study Methods

The apparent surface tension (γ) of LHRH and its analogues was measured using a Fisher Autotensiomat (Model 215) and a 6-cm platinum ring. Control experiments demonstrated that at least 3 ml of solution was required for precise γ measurements when using a 6-cm ring. Sample solutions containing 0.01 M total buffer were allowed to equilibrate for several minutes before taking the final reading in triplicate. In experiments where γ changed with time, γ was taken at known time intervals using the point of ring release as the recorded time.

Peptide liquid crystal melting temperatures (T_{cm}) were determined by loading peptide solutions into flat, glass capillary tubes ($50 \times 3 \times 0.3$ mm, Vitro Dynamics Inc., NY) and examining them microscopically ($33\times$) under crossed polar-

ized light. Typically solutions were prepared at least 24 hr prior to examination. Liquid crystals, when observed through crossed polars, were detected as light-colored structures of nondistinct crystal form against a black background (nematic liquid crystals of undulose extinction). Both nafarelin and detirelix showed an observed optical retardation of ~ 50 – 200 nm/0.3 mm, corresponding to a birefringence of ~ 0.001 or less as calculated using the Michel-Levy chart (11,12). The extent of birefringence was verified by viewing through a "first-order red" plate compensator; by this method the liquid crystals were characterized by the second-order blue (addition) and first-order yellow-orange (subtraction) colors. In most cases, photomicrographs were taken such that both the air (the concave side of the meniscus) and the solution regions were observed so as to provide an optical control for birefringence caused by imperfections in the microslide. The effect of temperature was determined by heating the microslides at $3^{\circ}\text{C}/\text{min}$ until all traces of liquid crystallinity were lost, i.e., until the background turned completely black. This melting temperature is defined herein as the critical melting temperature (T_{cm}).

Freeze-fracture electron micrographs were produced by flash-freezing an aqueous solution of detirelix to -80°C in liquid freon and then cooling to -196°C in liquid nitrogen. Samples at -196°C were then fractured by means of a cooled blade and etched and shadowed with platinum and carbon. Replicates were obtained by dissolving the sample in methanol and were then viewed by transmission electron microscopy.

RESULTS AND DISCUSSION

Temperature and pH Dependence on Native LHRH Degradation. This was determined at 60, 80, and 100°C by reversed-phase HPLC analysis. All reactions obeyed pseudo-first-order kinetics over the time courses studied (Fig. 2). The observed pseudo-first-order rate constants shown in Table I and Fig. 3 indicate that the degradation of LHRH is both acid and base catalyzed. The slope of -1 in the acid region is indicative of specific acid catalysis by hydronium ion. In the base region, the observed rate is not stoichiometrically proportional to hydroxide ion concentration but displays a slope of ~ 0.64 . The pH rate profiles obeyed the semiempirical rate equation given by Eq. (1), where k_{H^+} , k_o , and k_{HO^-} are the secondary rate constants for catalysis by hydronium ion, water (or a spontaneous

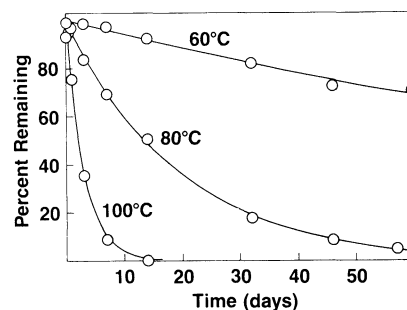


Fig. 2. Degradation of native LHRH in pH 6.3 buffer at 60, 80, and 100°C. The first order fit of the data was made by nonlinear least-squares analysis.

Table I. Observed Rate Constants for the Degradation of LHRH in Aqueous Solution

Buffer ^a	60°C		80°C		100°C	
	pH ^b	10 ⁷ k _{obs} (sec ⁻¹)	pH ^b	10 ⁶ k _{obs} (sec ⁻¹)	pH ^b	10 ⁵ k _{obs} (sec ⁻¹)
HCl	1.11	270	1.12	110	1.12	38
HCl	3.80 ^c	0.58	3.80 ^c	0.30	3.80 ^c	0.16
Acetate	4.45	0.39	4.52	0.23	4.53	0.12
Acetate	5.43	0.42	5.51	0.30	5.53	0.20
Phosphate	6.27	0.71	6.30	0.59	6.30	0.38
Phosphate	7.64	2.8	7.65	3.2	7.60	2.8
Carbonate	9.64	63	9.48	55	9.36	24

^a Total buffer concentration (except HCl solution), 0.01 M; ionic strength, $\mu = 0.15$.

^b pH's were determined at the reaction temperature indicated except for 100°C, where pH's were obtained from linear least-squares analysis of $1/T$ (K⁻¹) vs pH.

^c The pH before addition of LHRH acetate salt was ~ 3.02 .

$$k_{\text{obs}} = k_{\text{H}^+} a_{\text{H}^+} + k_{\text{o}} + k_{\text{HO}^-} (a_{\text{HO}^-})^x \quad (1)$$

reaction), and hydroxide ion, respectively. The terms a_{H^+} and $(a_{\text{HO}^-})^x$ are the hydronium ion and hydroxide ion activities, where the exponent x represents the observed dependence of the reaction rate upon hydroxide ion activity. As suggested earlier for nafarelin (7) a slope of less than one in the basic region indicates that LHRH degrades by several different basic pathways, each with its own pH dependence and true k_{HO^-} catalytic coefficient. The rate data at 60–100°C were fitted by nonlinear least-squares analysis (13) to Eq. (1) using a four-parameter fit: k_{H^+} , k_{o} , k_{HO^-} , and x . The best-fit value of x did not vary significantly over the temperature range studied ($x = 0.65 \pm 0.05$, 0.65 ± 0.03 , and 0.61 ± 0.03 at 60, 80, and 100°C, respectively), showing that a single value of x ($x \sim 0.64$) can be used without oversimplification to obtain the rate constants k_{H^+} , k_{o} , and k_{HO^-} by Eq. (2).

$$k_{\text{obs}} = k_{\text{H}^+} a_{\text{H}^+} + k_{\text{o}} + k_{\text{HO}^-} (a_{\text{HO}^-})^{0.64} \quad (2)$$

The secondary rate constants obtained by this method are shown in Table II, as are the corresponding activation parameters. The rate constants at 25°C were estimated by

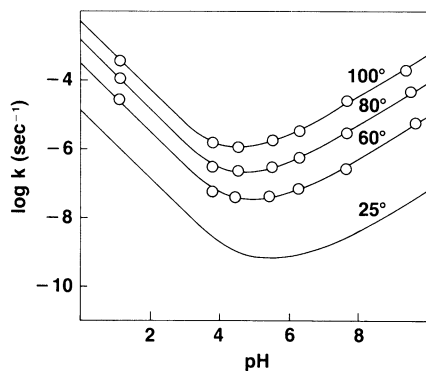


Fig. 3. pH–rate profiles for the degradation of native LHRH at 60–100°C. The lower dashed line is the pH–rate profile for 25°C calculated using Eq. (2) and the activation parameters obtained from the data at 60–100°C.

linear least-squares extrapolation of the Arrhenius data; the lower line in Fig. 3 is the best fit of the calculated 25°C rate constants to Eq. (2).

Two features are readily apparent: (i) the pH of maximum stability for native LHRH (and probably structurally similar LHRH analogues as well) at 25°C is near pH 5.4, and (ii) native LHRH exhibits a shelf life of 2 years or more from pH ~ 4.2 to ~ 7.2 . Comparison of these rate data with those reported earlier for nafarelin (7) and RS-26306 (8) shows that there is little difference in chemical stability between native LHRH and some of its hydrophobic analogues. This broad plateau region suggests that the spontaneous (or water-catalyzed) reaction for LHRH degradation largely determines drug stability from pH 4 to pH 7. Additionally, reaction solutions of pH ~ 2.5 to ~ 9.5 show less than 10% degradation after 1 month, well within the time required to carry out the peptide liquid crystal studies herein.

Surfactant Nature of Nafarelin and Detirelix. This was probed by determining their apparent surface tension (γ) of aqueous peptide solutions at 25°C. A cursory glance at the structures in Fig. 1 shows that detirelix and nafarelin should be more surface active than native LHRH. At neutral pH detirelix has two protonated aminoacids (arginine and diethyl homoarginine) which are close to the N terminus, making this end hydrophilic. Near the C terminus, detirelix has several large organic aminoacids (naphthylalanine, *p*-chlorophenylalanine, tryptophan, and tyrosine), making this end lipophilic (14). The aggregation of amphiphiles is known to be driven by “opposing forces” of attraction of the lipophilic regions and geometrical packing constraints, the balance of which is responsible for the characteristics and maintenance of subsequent structures (15). Detirelix and nafarelin have such lipophilic and hydrophobic regions, making them both surface active and highly susceptible to aggregation in aqueous solution.

The apparent surface tension of detirelix in pH 7.4 phosphate buffer showed a classical (15) γ versus $\log[\text{peptide}]$ profile (Fig. 4), giving from the sharp change in slope a critical micelle concentration (CMC) of 5.3×10^{-4} M (0.88 mg/ml). The limiting slope below the CMC, $\partial\gamma/\partial\log[\text{peptide}]$, is ~ 6.6 mN m⁻¹, providing via the Gibbs equation [Eq. (3)] a surface excess concentration (Υ) of 1.16×10^{-6} mol m⁻².

$$\Lambda = \frac{1}{2.303 RT} \frac{\delta\gamma}{\delta\log[\text{peptide}]} \quad (3)$$

Using Eq. (4), where N_{A} is Avogadro's number, the calculated surface area/molecule (A) is 1.43 nm².

$$A = 1/(N_{\text{A}}\Upsilon) \quad (4)$$

Inspection of Fig. 4 shows that γ for nafarelin also decreases with increasing nafarelin concentration at pH 7.4. The slope of this plot is 9.8 mN m⁻¹, giving $\Upsilon = 1.7 \times 10^{-6}$ mol m⁻² and a surface area/molecule of 0.97 nm². The surface area per molecule for nafarelin is slightly smaller than for detirelix, presumably because of the different head group size. It is known that the size of the hydrophilic head group, rather than the size or the length of the lipophilic chain, affects the value of Υ (16–19). Nafarelin has a hydrophilic region consisting of the sequence Gly–Pro–Arg, whereas detirelix has a slightly greater hydrophilic region, consisting of

Table II. Secondary Rate Constants and Activation Parameters for the Degradation of LHRH in Aqueous Solution^a

Rate constant	Temperature				Activation parameters (ΔH^\ddagger , kcal mol ⁻¹) (ΔS^\ddagger , cal K ⁻¹ mol ⁻¹)
	25°C	60°C	80°C	100°C	
k_H (M ⁻¹ sec ⁻¹)	1.4×10^{-5b}	3.0×10^{-4}	1.3×10^{-3}	5.0×10^{-3}	$\Delta H^\ddagger = 16.6$ $\Delta S^\ddagger = -25.0$
k_0 (sec ⁻¹)	5.3×10^{-10b}	2.5×10^{-8}	1.4×10^{-7}	8.3×10^{-7}	$\Delta H^\ddagger = 20.8$ $\Delta S^\ddagger = -30.9$
k_{HO^-} (M ^{-0.64} sec ⁻¹) ^c	2.5×10^{-5b}	8.5×10^{-4}	5.0×10^{-3}	2.2×10^{-2}	$\Delta H^\ddagger = 19.3$ $\Delta S^\ddagger = -14.8$

^a Calculated using Eq. (2) (see text). The values of K_w used in calculating a_{HO^-} from the pH's at 25, 60, 80, and 100°C were 14.0, 13.02, 12.60, and 12.29 M⁻¹, respectively.

^b Calculated from the activation parameters shown in the last column.

^c The secondary rate constants for hydroxide ion catalysis demonstrated a 0.64 exponent dependence on hydroxide ion concentration, and so the value of k_{HO^-} has the units of M^{-0.64} sec⁻¹. Fortunately, this does not detract from its usefulness in calculating the pH-rate profile at 25°C.

Gly-Pro-Arg-Leu-(homodiethyl Arg). Further, the CMC for nafarelin is greater than 2 mg/ml, somewhat higher than for detirelix, presumably because nafarelin has a weaker lipophilic attraction than detirelix, or because the larger head group size for detirelix prevents close packing of the peptide monomers to give micelles and higher ordered structures.

Liquid Crystal Formation. The liquid crystal formation of nafarelin and detirelix was studied by freeze-fracture electron microscopy and by examination under crossed polarized light using optical microscopy. Upon freeze-fracture analysis, concentrated solutions of detirelix (for example, 15 mg/ml as shown in Fig. 5) formed lyotropic mesophases, indicating a marked ordering of drug in solution. Similar freeze-fracture replicates were also observed for nafarelin solutions but were absent in control solutions containing only buffer (data not shown). Structural ordering of this type has been observed previously, for example, in freeze-fracture replicates of emulsions and creams (20). Peptide aggregation in other peptides and proteins has also been reported, for example, for pentagastrin (21) and insulin (22).

Birefringence due to liquid crystal formation in aqueous nafarelin and detirelix solutions was determined by sample observation under crossed polars. Although measurement of birefringence is a sensitive method for the detection of liquid crystals, the extent of birefringence is difficult to quantify, especially because of its time-dependent nature and unknown relation to the extent or thermodynamic stability of

the peptide liquid crystal structures. Herein we have chosen the critical melting temperature (T_{cm}) as an indicator for characterizing peptide liquid crystals. In general, T_{cm} was independent of liquid crystal maturation (Fig. 6) and increased only slightly with increasing peptide concentration (Figs. 7 and 8). In the absence of added electrolyte, detirelix and nafarelin did not form liquid crystals at concentrations below 4 and 8 mg/ml, respectively. That detirelix formed liquid crystals at a lower concentration than nafarelin is in keeping with Tanford's suggestion (15) that hydrophobic self-association is the driving force behind aggregate formation—by this criterion detirelix is more hydrophobic than nafarelin (Fig. 1). This is also supported by our observation that the hydrophilic parent peptide, native LHRH, did not exhibit birefringence or anisotropy, even at 30 mg/ml LHRH in 1 M NaCl solution. Under these extreme conditions both nafarelin and detirelix gel immediately, indicative of their hydrophobic nature as compared with native LHRH.

Thus, both indirect (surface activity and determination

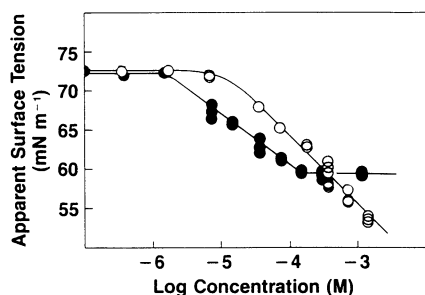
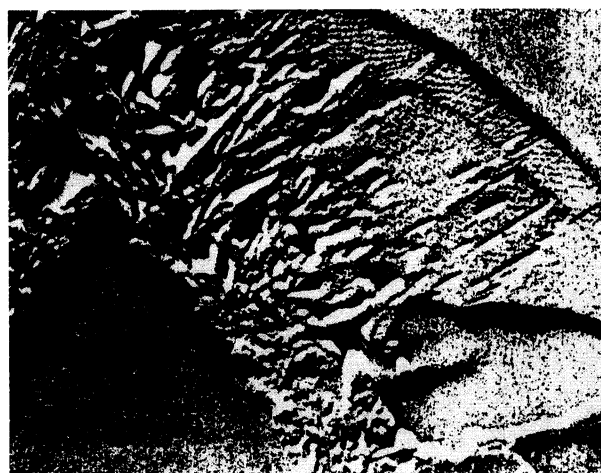


Fig. 4. Effect of detirelix (●) and nafarelin (○) concentration on the apparent surface tension (γ) at 25°C. The sharp break at 5.3×10^{-4} M is the critical micelle concentration for detirelix in 0.01 M phosphate buffer (pH 7.4).



← 300 nm →

Fig. 5. A freeze-fracture replicate of detirelix in aqueous solution (15 mg/ml) as viewed by transmission electron microscopy. Control electron photomicrographs (not shown) without added peptide did not exhibit the ordered array in this figure.

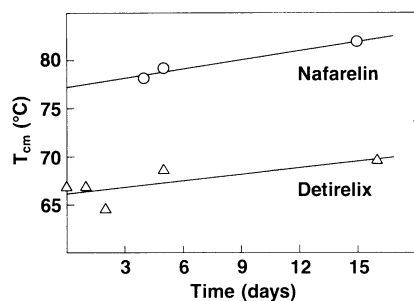


Fig. 6. Effect of reaction time on the critical melting temperature (T_{cm}) of nafarelin (18.8 mg/ml) and detirelix (19.9 mg/ml) solutions. Generally, a slight increase was noted, however, it is not considered large enough to complicate the cosolvent addition results presented herein (vide infra).

of CMC) and direct measurements (optical observation) demonstrate that hydrophobic LHRH analogues aggregate readily in aqueous solution. Because the aggregation of detirelix and nafarelin has important pharmaceutical consequences, particularly in the design of peptide parenteral formulations, the remainder of this paper describes how liquid crystal formation may be suppressed by added cosolvent.

Peptide Liquid Crystals. These were disrupted by adding organic cosolvent where, in general, increasing amounts of propylene glycol (PG) and higher temperatures suppressed the formation of peptide liquid crystals. Inspection of Fig. 7 shows that added PG reduced T_{cm} , particularly above 10–15% PG. [Similar decreases in T_{cm} have been reported previously, for example, by the addition of glycerol or ethylene glycol to disodium cromoglycate/water systems (23)]. The lack of liquid crystals in nafarelin solutions containing more than 15% PG (w/v) may be due to (i) a reduction in T_{cm} to room temperature, thus preventing liquid crystal formation on a thermodynamic basis, or (ii) a large kinetic barrier, resulting in the slow formation of nafarelin liquid crystals in the presence of excess PG. This latter rationale is supported by the long and variable lengths of time required to induce nafarelin liquid crystal formation, even for nafarelin solutions without added PG.

Detirelix exhibited lower T_{cm} 's than nafarelin (Fig. 8), indicating that detirelix liquid crystals are less stable than nafarelin liquid crystals at elevated temperatures (40–80°C). This is somewhat surprising inasmuch as (i) detirelix exhibits a lower CMC (0.88 mg/ml) than does nafarelin, (ii) detirelix at 10 mg/ml or greater readily forms liquid crystals in less than 1 hr, whereas nafarelin often takes more than 1 week,

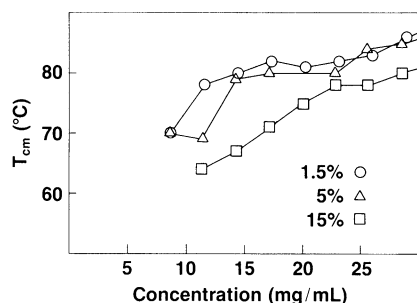


Fig. 7. Effect of PG (% w/v) as added cosolvent on the critical melting temperature (T_{cm}) of nafarelin liquid crystals.

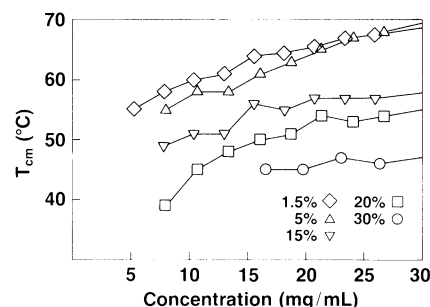


Fig. 8. Effect of PG (% w/v) as added cosolvent on the critical melting temperature (T_{cm}) of detirelix liquid crystals.

and (iii) detirelix forms liquid crystals at a lower concentration (~4 mg/ml) than nafarelin (~8 mg/ml). The higher T_{cm} 's for nafarelin demonstrates that there exists a balance between kinetic and thermodynamic forces affecting the formation and stability of peptide liquid crystals. These results indicate that, even though nafarelin forms liquid crystals slowly, once formed they are more stable. Such an observation is a breakdown of the Hammond postulate (a positive correlation between ΔG° and ΔG^\ddagger), a tenet of chemistry that, unfortunately, has many exceptions.

CONCLUSIONS

Comparison of the pH–rate data herein for native LHRH with data reported earlier for nafarelin (7) and RS-26306 (8) demonstrates that hydrophobic modification of LHRH has little effect on chemical stability. In contrast, the hydrophobic nature of certain LHRH decapeptides such as nafarelin and detirelix gives rise to unusual solution dynamics, including peptide aggregation and liquid crystal formation. These liquid crystals eventually result in solution gelation, with the ramification of compromised formulation elegance and utility. We have demonstrated herein that a pharmaceutically acceptable cosolvent, propylene glycol, raises the minimum concentration for peptide aggregation, and thus, many of the potential problems associated with aggregate formation may be minimized or eradicated by cosolvent addition.

ACKNOWLEDGMENTS

We are indebted to Nancy Benson, Department of Electron Microscopy, University of California, Berkeley, for the production of freeze-fracture replicates and to Dave Johnson, Jeff Fleitman, Peter Mishky, Katrina Herb, and John Nestor for their help and comments.

REFERENCES

1. S. T. Anik and J.-Y. Hwang. Adsorption of D-Nal(2)⁶LHRH, a decapeptide, onto glass and other surfaces. *Int. J. Pharm.* 16:795–801 (1983).
2. A. Rogerson and L. M. Sanders. Some solution properties of two decapeptides. *Proc. Int. Symp. Control. Rel. Bioact. Mater.* 14:97–98 (1987).
3. J. A. Feldman, M. L. Cohn, and D. Blair. Liquid chromatographic analysis of adriamycin and metabolites in biological fluids. *J. Liq. Chromatogr.* 1:833 (1978).
4. K. Nishi, H. Ito, S. Shinagawa, C. Hatanaka, M. Fujino, and

Explore Litigation Insights

Docket Alarm provides insights to develop a more informed litigation strategy and the peace of mind of knowing you're on top of things.

Real-Time Litigation Alerts



Keep your litigation team up-to-date with **real-time alerts** and advanced team management tools built for the enterprise, all while greatly reducing PACER spend.

Our comprehensive service means we can handle Federal, State, and Administrative courts across the country.

Advanced Docket Research



With over 230 million records, Docket Alarm's cloud-native docket research platform finds what other services can't. Coverage includes Federal, State, plus PTAB, TTAB, ITC and NLRB decisions, all in one place.

Identify arguments that have been successful in the past with full text, pinpoint searching. Link to case law cited within any court document via Fastcase.

Analytics At Your Fingertips



Learn what happened the last time a particular judge, opposing counsel or company faced cases similar to yours.

Advanced out-of-the-box PTAB and TTAB analytics are always at your fingertips.

API

Docket Alarm offers a powerful API (application programming interface) to developers that want to integrate case filings into their apps.

LAW FIRMS

Build custom dashboards for your attorneys and clients with live data direct from the court.

Automate many repetitive legal tasks like conflict checks, document management, and marketing.

FINANCIAL INSTITUTIONS

Litigation and bankruptcy checks for companies and debtors.

E-DISCOVERY AND LEGAL VENDORS

Sync your system to PACER to automate legal marketing.